

Optimization of key link parameters and mechanism of the jet-stirring synergistic column flotation method

Lingling Wang, Jinbo Zhu, Wei Zhou, Haoyu Wang, Shujie Wang

School of Materials Science and Engineering, Anhui University of Science and Technology, Huainan 232001, China

Corresponding author: awaly@126.com (Wei Zhou)

Abstract: In recent years, with the deepening of the degree of coal mining and the improvement of the mechanization and intelligent level of coal dressing, the proportion of fine and micro-fine coal production has been increasing. Micro-fine grade separation has gradually become an important research direction in coal washing industry. This paper is based on a novel jet-stirring synergistic column flotation method, which integrates jet-impact mixing, impeller mixing, and dispersion into the structure of a column flotation tank. By combining with existing research foundations, we construct a corresponding physical model and conduct optimization studies on key parameters related to jetting, impeller mixing, and mechanism. The resulting fundamental theory provides clear insights for the engineering application of this innovative flotation technology. The effects of jet-stirring synergy on bubble adsorption and reagent adsorption were studied, and the flotation effect of the new flotation technology was experimentally verified, laying a theoretical foundation for the industrial application of the device.

Keywords: coal slurry flotation, flotation unit, jet-stirring synergy, parameter optimization

1. Introduction

The National Bureau of Statistics released the "People's Republic of China 2023 National Economic and Social Development Statistics Bulletin" shows that in 2023, China's total energy consumption was 5.72 billion tons of standard coal, and the consumption of coal accounted for 55.3% of the total energy consumption (National Bureau of Statistics, 2024). Coal still occupies a dominant position in China's primary energy production and consumption, and is still a major part of the country's energy structure, and it continues to play the role of a bottom-up guarantee (Zhang et al., 2019; Zhang et al., 2021; Guo et al., 2015; Ge et al., 2023; Wang et al., 2023; Zhou, 2023).

In recent years, with the increasing degree of coal mining mechanization and intelligence, the scale of coal mining has been expanded, the coal from the coal beds with poor geological conditions has been mined, resulting in a decline in coal quality, and the proportion of fine-grained and micro-fine-grained coal output is also higher and higher, and micro-fine-grained sorting has gradually become a hot research direction in the coal beneficiation industry (Sun et al., 2020; Yuan 2017; Miao and Qian, 2009; Yang et al., 2021). Fine-grained coal slurry with a particle size of 0.5 mm or less is usually sorted by flotation. Today, coal slurry flotation generally uses non-polar hydrocarbon oil (such as paraffin, diesel, etc.) as the collector, these oils are insoluble in water and need to be fully dispersed under the action of mechanical or non-mechanical forces to achieve full adsorption of flotation agents on the surface of coal particles, enhance the hydrophobicity of coal particles, and provide good initial conditions for subsequent flotation operations. This dispersion work needs to be done in the slurry mixing process before flotation (Xia et al., 2019; Huang et al., 2022; Li et al., 2019; Li et al., 2010; Zhu, 2022). Due to the lack of in-depth understanding of slurry regulation mechanism, and the current coal slurry flotation is still dominated by long process, the actual operation of the slurry regulation link management is insufficient, only through the subsequent continuous multi-cell flotation equipment to make up for the slurry regulation effect. In fact, to give full play to the efficiency of flotation equipment, it is necessary to provide the best initial conditions for the entire flotation process, which must strengthen the

conditioning of the pulp before flotation. Currently, the main pulp adjustment methods are mechanical mixing pulp adjustment, jet shear pulp adjustment, pressure pulp adjustment, electrochemical pulp adjustment and ultrasonic pulp adjustment (Li et al., 2014). Among them, pressure sizing method, electrochemical sizing method and ultrasonic sizing method have not been widely used because of the limitation of use conditions. Mechanical mixing slurry regulation method is the most traditional, this method is the direct use of impeller stirring on the flotation machine to achieve the dispersion of chemicals, widely used in fine mineral flotation; Jet shear slurry regulation method is mainly used in suction and agitation of flotation process, and has good effect on flotation reagent dispersion, bubble dispersion and drug gas uniform dispersion, and has the advantages of arranging along the slurry conveying pipe and adjusting slurry for a long time, so it is a hot research direction at present (Xu et al., 2023; Safari et al., 2020; Schwarz et al., 2019; Shi et al., 2006; Bu et al., 2021; Wang et al., 2021). In the working process of the jet device, the air is rolled up and dissolved, shear dispersion into tiny bubbles, the pharmaceutical adheres to the surface of the bubble liquid film, and the mineral particles collision adhesion, creating a strong multi-phase coupling effect. However, the single jet beam stirring force is weak, and the dispersion uniformity of multiphase fluid in the flotation tank is poor (Wang et al., 2020; Li et al., 2020; Zhu et al., 2019; Han et al., 2019; Wang, 2019). It can be seen that coal slurry flotation and slurry conditioning within the flotation equipment is a multi-scale multiphase mixing and inter-particle collision adhesion process. In contrast, the single stirring flotation flow field within the traditional flotation equipment becomes a bottleneck limiting the further improvement of flotation/slurry conditioning.

In order to improve the effect of flotation slurry conditioning, strengthen the coal slurry conditioning and flotation process synchronously, give full play to the advantages of the jet, impeller mixing, and column flotation fields. A jet-stirring synergistic column flotation process combining jet-stirring mixing, impeller mixing and dispersion with column flotation countercurrent collision is proposed. In order to strengthen the slurry conditioning and flotation processes simultaneously, the advantages of the jet flow field, impeller stirring flow field and column flotation flow field should be fully utilized, and the mechanism of simultaneous strengthening of slurry conditioning and flotation processes should be explored from the perspective of synergistic action of multi-dimensional mixing and dispersing modes of jet suction, impeller stirring and column flow field, to form a new flotation technology with clear basic theories and feasible engineering applications. The jet-stirring synergistic column flotation process is shown in Fig. 1-1.

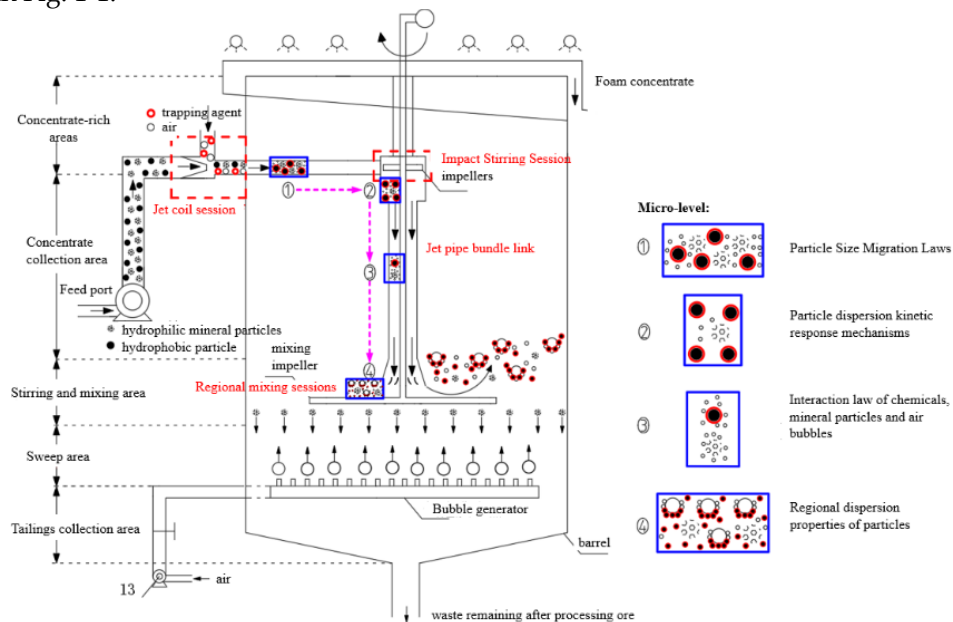


Fig. 1-1. Process of jet-stirring synergistic column flotation

The process combines the movement modes of jet coiling suction, impact mixing, stirring diffusion and countercurrent collision together, breaking through the traditional flotation device with a single jet or mechanical stirring movement mode, combining the technical advantages of high flow ratio of jet

mixing, high dispersion of impeller stirring and low turbulence of column countercurrent collision to strengthen the slurry mixing/flotation process. The essence of the process is the multi-scale multi-phase mixing movement, collision adhesion between particles, interfacial interaction, and interface interaction. This process involves many complex micro-scientific issues, one of the core issues is the jet-stirring synergistic effect of the agent and its carrier bubbles suction dispersion, mixing flow law, and the other is collision and adhesion law of the agent, coal slurry, bubbles and other multi-phase particles in the synergistic flow field. The in-depth study of these issues is the key to further reveal the synergistic action of jetting and stirring to enhance the coal slurry column slurry adjustment/flotation process.

On the base of above study, combined with this jet-stirring synergistic column flotation method, this paper builds the corresponding physical model, and proposes to carry out the optimization of the key parameters of jet, impeller stirring and column, so as to form a new flotation technology with clear basic theory and engineering application. Numerical simulation under the unilateral and synergistic effects of jet, stirring and column link was carried out to optimize the structural parameters of the key link, and investigate the influence of jet-stirring synergy on the adsorption of chemicals; experimental verification of the flotation effect of coal slurry adjustment was carried out, which lays the theoretical foundation for the industrial application of the device; the basic theory of the existing coal slurry flotation/pulp adjustment was enriched and the basic theory of the jet-stirring synergistic column flotation/pulp adjustment was developed. It is of great theoretical significance and practical value to enrich the basic theory of existing coal slurry flotation/slurry and provide theoretical support for the further improvement and industrial application of jet-stirring synergistic column flotation/slurry adjustment process.

2. Numerical simulations of key aspects of jet-stirring synergistic column flotation device

The working process of the jet-impact mixing device is mainly divided into two parts, one is the full suction mixing of the jet mixing device for the ejected fluid, and the other is the mixed fluid impact impeller, using the impeller stirring and shearing effect and jet suction to promote the suction and homogeneous mixing of the ejected fluid in the device. Based on this, a single jet mixing device, impact mixing device, and jet-impact mixing device three-dimensional model were constructed, and the relevant literature was consulted to determine the type of model structural parameters and a reasonable range of values. Three kinds of numerical simulations of the flow field were carried out to obtain the distribution of the gas ejection under different jet parameters and flow conditions. The distribution of gas ejection under different jet parameters and flow field conditions was obtained by numerical simulation.

2.1. Numerical simulation of jet-impact stirring synergistic link

2.1.1. Model construction

The working process of the jet-impact mixing device is divided into two parts: the jet roll suction mixing (primary mixing), and the mixed fluid impact impeller stirring mixing (secondary mixing). The optimization of the parameters of the jet mixing device has been completed in the previous period, and the structural parameters of the jet mixing device are no longer studied, and the types and values of its fixed parameters are determined by reviewing the relevant literature. In the process of the jet-impact mixing device volume suction gas, the primary mixing part of the variable parameters affecting the mixing of the working fluid and the elicited fluid to choose the intensity of the jet (characterized by the nozzle exit velocity v) and the throat length L_h ; the secondary mixing part of the impeller is a passive rotating, affecting the mixing of the working fluid and the elicited fluid to choose the variable parameters of the working fluid and elicited fluid mixing with or without the impeller and impeller filling degree (Impeller diameter D_s and chamber diameter D_q ratio). Practical production applications, rely solely on the impact of the jet beam is often difficult to make the impeller uniform and stable passive rotation, so in the simulation of the jet-impact mixing synergistic flow field, variable parameters to increase the speed of an impeller, simulation of its rotation and the jet device synergistic device volume suction mixing capacity of the impact of the device.

The fixed structural parameters in the jet mixing device are reduced to the optimal values in the literature (Zhou, 2019). The fixed structural parameters in the jet mixing device are as follows, the

variable structural parameter is the length of the throat, the variable structural parameter of the impact mixing part is the diameter of the impeller, and the values and ranges of the specific parameters are shown in Table 2-1.

Table 2-1. Parameters value of jet-impact stirring device

Parameter type	Parameter name	Range of values	Final value
Fixed structural parameters	Nozzle Diameter D_z /mm	Area ratio	10
	Laryngeal Diameter D_h /mm	$A_r = \left(\frac{D_h}{D_z}\right)^2 = 1.96\sim 3.24$	18
	Glottal spur L_e /mm	$L_e = 0.3D_h \sim 0.6D_h$	10
	Nozzle convergence angle α /°	14°~16°	15
	Laryngeal diffusion angle β /°	Determined by working conditions	0
	Diameter of feeding tube D_r /mm	Determined by working conditions	30
	Diameter of ejector tube D_y /mm	Determined by working conditions	5
	Suction tube position	/	Front-to-back nozzles, symmetrical arrangement
	Number of impeller blades N	4~8	6
	Chamber Diameter D_q /mm	Determined by working conditions	120
	Chamber outlet diameter D_c /mm	Determined by working conditions	70
	Variable structural parameters	Impeller diameter D_s /mm	50~110
Laryngeal length L_h /mm		$>9D_z$	$n * D_z$ ($n > 9$, take an integer)

According to the value scheme listed in the above table, the model structure parameters are finally determined: area ratio $A_r = 3.24$ ($D_h = 18$ mm, $D_z = 10$ mm), $L_e = 0.56$, $D_h = 10$ mm, the pilot tube is symmetrically arranged in front of the nozzle and bilaterally, with the diameter of 5 mm, and the angle of convergence of the nozzle is $\alpha = 15^\circ$. In order to reduce the velocity attenuation of the jet beam in the throat before impacting on the impeller, the diffusion tube is canceled, that is, the diffusion angle $\beta = 0^\circ$ for the throat is taken as the value required for calculation. In order to reduce the velocity attenuation of the jet beam before impacting the impeller, the diffusion tube is canceled, i.e., the diffusion angle of the tube $\beta = 0^\circ$, and the length of the tube L_h is taken according to the calculation. Initial working fluid feeding velocity $v_g = 2$ m/s, according to the formula can be calculated nozzle exit velocity $v = 18$ m/s, the initial velocity of the pilot tube inlet is 0 m/s, and the relative pressure is 0 MPa.

Based on the structural principle of the jet-impact stirring mixing device, Solid Works software and Ansys Workbench (version 2022R1) were used for modelling and model pre-processing, meshing, solution calculations and data post-processing, respectively. The jet coiling and suction section, the impact stirring section and the jet-impact stirring synergistic section are modelled and the fluid domain is determined. Since the impact stirring part includes the impact stirring impeller, it is necessary to establish the rotation domain around the impeller when modeling, and divide two separate watersheds Fluid1 and Fluid2 to facilitate the subsequent setting of the motion conditions; the rotation of the impeller adopts the dynamic mesh method, and the 6-degree-of-freedom option is ticked, and the region where the impact stirring impeller is located, Fluid2, is the rotation domain, and it is set up as the rotation of the impeller, and Fluid1 is set up to rotate with the motion. Rotation. The three models are shown in Fig. 2-1, Fig. 2-2 and Fig. 2-3 respectively.

2.1.2. Meshing

Mesh types include structured and unstructured meshes, commonly used structured meshes are quadrilateral, hexahedral meshes and unstructured meshes are triangular and tetrahedral meshes. The model is automatically meshed using the Ansys meshing module. The finer the mesh division and the higher the number, the more accurate the solution calculation in general, but due to the limitations of the calculation conditions and the consideration of the impact of time cost, the number of mesh divisions should be within a reasonable range. As shown in Figs. 2-4, 2-5 and 2-6, the grid size of the jet chamber is 1mm, the pilot tube is 0.6mm, the throat is 1mm, the impact impeller is 0.5mm, the impeller sleeve is 10mm, and the total number of grid cells is 1076814.

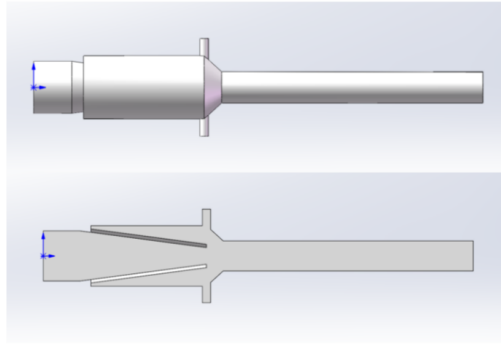


Fig. 2-1. Model of the jet mixing section

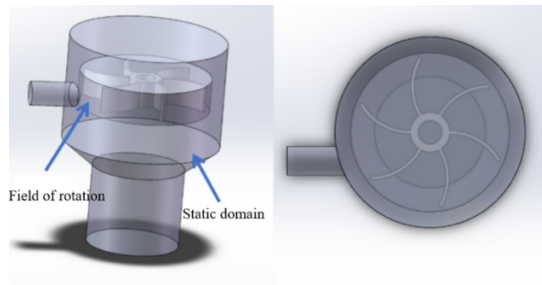


Fig. 2-2. Model of impact mixing section

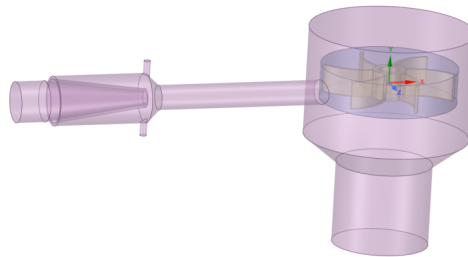


Fig. 2-3. Model of jet-impact mixing synergistic section

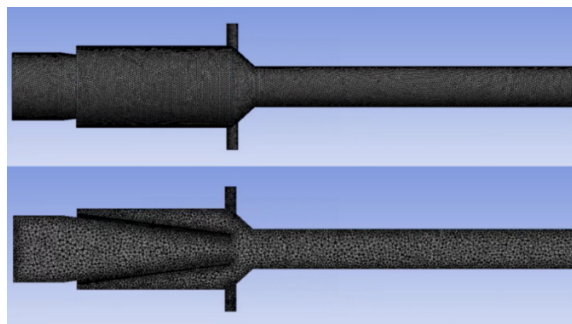


Fig. 2-4. Mesh division of jet mixing section

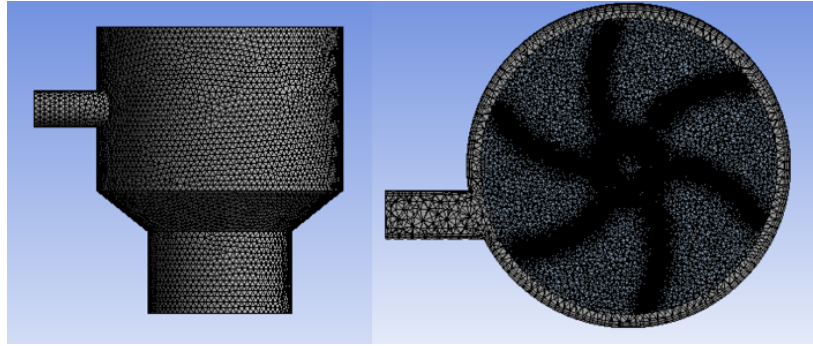


Fig. 2-5. Mesh division of stirring section

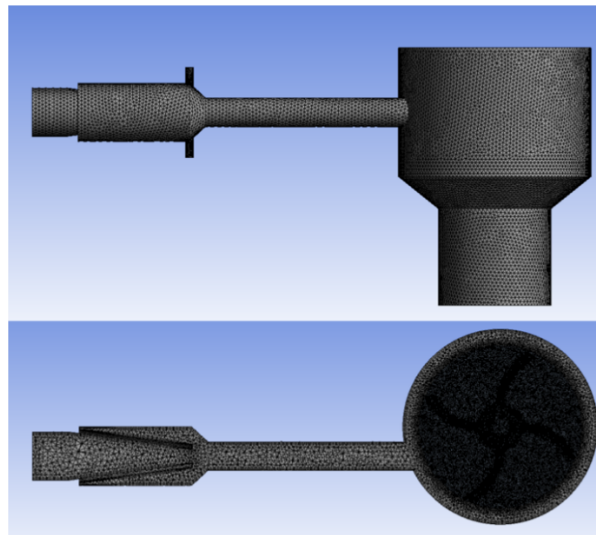


Fig. 2-6. Mesh division of jet-impact mixing synergistic section

2.1.3. Boundary condition setting

Simulations were carried out using the Fluent module in Ansys Workbench version 2022R1. The meshing module delineated the mesh, which was updated and imported into the solver, mesh checking was carried out, the unit of length was corrected to millimeter, and the unit of length of the flow region was set to millimeter.

Solver parameter setting: in the solver dialogue box, parameters such as model, material, cell area conditions, boundary conditions, are set in turn. For the jet mixing device, the pressure-based solver is selected, the second-order windward format is chosen for each parameter in the spatial discretization option, the coupling of velocity and pressure is adopted in the SIMPLEC mode, and the converged residuals are set to 10^{-4} , and the turbulent model is chosen to be the Realizable $k-\epsilon$ model in the $k-\epsilon$ model (2 eqn), and the wall function is chosen to be the Standard Wall Function (SWF). A realizable $k-\epsilon$ model in epsilon (2 eqn), and the standard wall function (SWF) is selected for the wall function. For the stirring component, the dynamic mesh needs to be set up, tick the 6 degrees of freedom option to set it up and create a dynamic mesh region. When a given velocity is required, use the Profile file to define the rotation of the impeller in the fluid domain, time to define the computation time, and ω_y to define the angular velocity.

Fluid material setting: add liquid water in the material module, density 1000 kg/m^3 , viscosity 0.001 MPa s , and set the priming fluid as air.

Boundary condition settings: the inlet of the inlet adopts the velocity inlet condition, and the inlet velocity is set to 2 m/s ; the inlet of the ejector tube inlet1 and inlet2 adopts the pressure boundary, and the relative pressure is set to 0 Mpa ; the outlet of the throat is set to the pressure boundary, and the wall is the non-slip boundary condition; the turbulence intensity and hydraulic diameter are selected in the

turbulence specification method item, and the Turbulence Intensity(%) keeps the default value of 5, and Hydraulic Diameter is set to 18 mm according to the actual modeling size.

After the calculation the results of the numerical calculations are data processed in the post-processing module CFD-post in Ansys Workbench.

2.2. Analysis of numerical simulation results

2.2.1. Influence of the jet link on the coiling and mixing capacity of the device

The fixed structural parameters of the model: area ratio $Ar = 3.24$ ($D_h = 18$ mm, $D_z = 10$ mm), $Le = 0.56D_h = 10$ mm, the diameter of the ejector tube is 5 mm, bilaterally symmetrical arrangement, angle of convergence of the nozzle $\alpha = 15^\circ$, and diffusion angle $\beta = 0^\circ$ of the throat. The length of the throat was $L_h = 150$ mm, the initial velocity at the inlet of the ejector tube was 0 m/s, and the relative pressure was 0 MPa.

2.2.1.1. Influence of jet strength on the ability of the device to direct fire

The structural parameters of the model remain unchanged, the working fluid is set to be water, and the induced fluid is set to be air, and the intensity of the jet is changed by changing the feeding velocity v_g of the model inlet boundary condition, so that the nozzle exit velocity v varies from small to large, and v is adjusted to be 3.6 m/s, 7.2 m/s, 10.8 m/s, 12.6 m/s, 18 m/s, and 27 m/s, respectively, and the simulation is calculated for 3 s to explore the gas distribution law of the jet in the jet device to explore the coiling distribution law of the gas in the jet.

The cloud diagram of gas volume distribution under different nozzle outlet speeds is shown in Fig. 2-7. From the Fig., it can be seen that the nozzle exit velocity has a greater impact on the device suction mixing ability, when the nozzle exit velocity $v < 3.6$ m/s, the jet strength is small, the jet device suction dispersion ability is weak, the gas is mainly concentrated in the boundary of the jet beam, which is not conducive to the bubble rupture and dispersion; when the nozzle exit velocity 7.2 m/s $< v < 18$ m/s, with the increase of the jet velocity, the gas volume fraction of the same cross-section position increases. When the nozzle exits velocity $v \geq 18$ m/s, the ejection ability of the jet device reaches the limit, and the volume fraction of the gas in the pipe no longer increases with the increase of jet velocity.

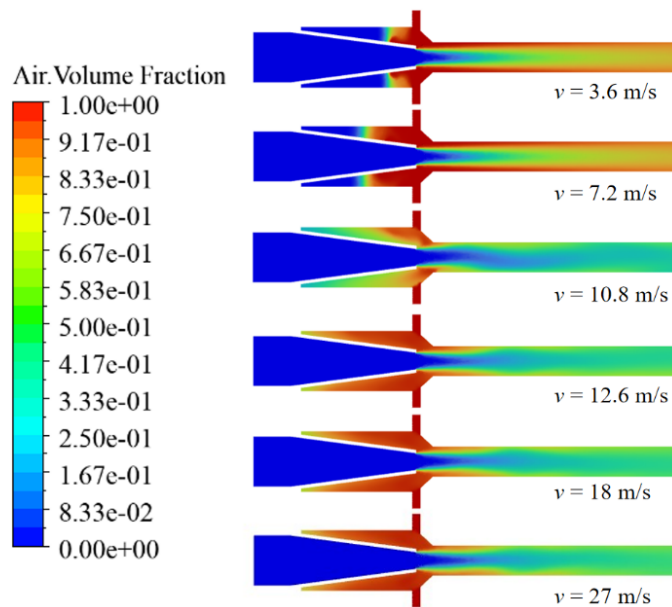


Fig. 2-7. Clouds of air volume fraction at different nozzle exit velocities

2.2.1.2. Effect of jet strength on the flow field

As shown in Fig. 2-8 for different nozzle exit velocity under the axial velocity cloud diagram, from the Fig. can be seen, the jet beam there is an axial velocity core area, and with the flow of the beam in the tube, the axial velocity gradually decreases; the larger the nozzle exit velocity, the larger the difference

in velocity between the ejected fluid and the working fluid, the stronger the ejection capacity of the device; when the nozzle exit velocity is large enough ($v \geq 18$ m/s), the difference in velocity between the two streams reaches a maximum. When the nozzle outlet speed is large enough ($v \geq 18$ m/s), the velocity difference between the two fluids reaches the maximum, at this time the device ejection capacity reaches the limit.

As shown in Fig. 2-9 for different nozzle exit velocity under the turbulence intensity map, from the Fig. can be seen, the jet device, the turbulence intensity of the largest change in the region for the nozzle exit, the two streams of fluid in the initial energy exchange, with the nozzle exit velocity increases, the turbulence intensity to enhance the jet beam into the back of the throat after the turbulence intensity is weakened, that is, at this time, the exchange of energy between the fluids has been basically completed.

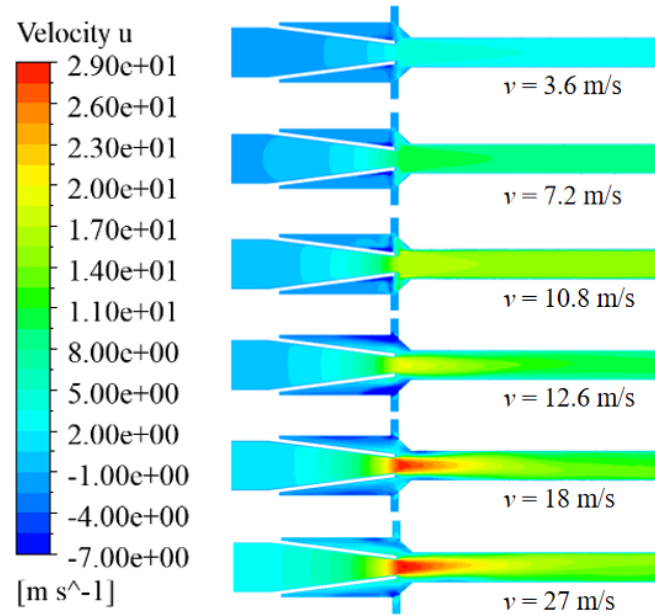


Fig. 2-8. Clouds of velocity u at different nozzle exit velocities

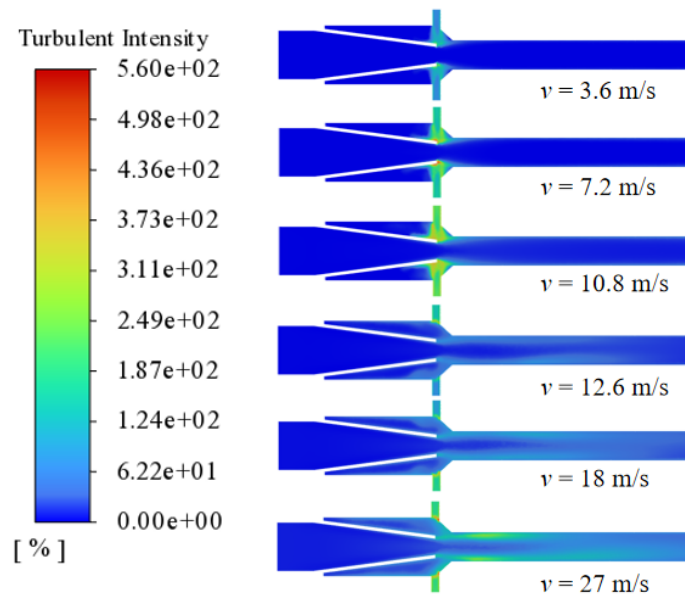


Fig. 2-9. Clouds of turbulent intensity at different nozzle exit velocities

As shown in Fig. 2-10 for different nozzle exit velocity under the axial static pressure cloud diagram, it can be seen from the Fig., the larger the nozzle exit velocity, the greater the negative pressure formed inside the mixing chamber, the more favourable to the volume attraction injection fluid; when the nozzle exit velocity is sufficiently large, the throat inlet will also form a negative pressure zone.

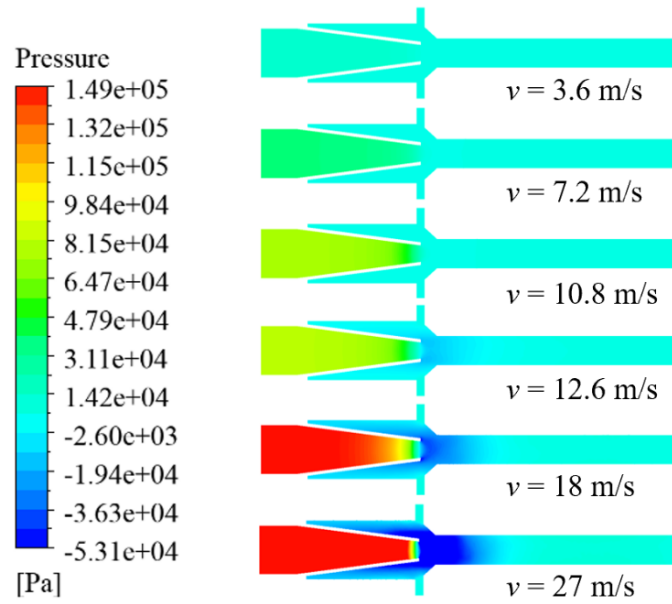


Fig. 2-10. Clouds of pressure at different nozzle exit velocities

2.2.1.3. Influence of throat length on device elicitation capacity

The rest of the parameters remain unchanged, only change the length of the throat, to explore the ability of the jet device volume suction of mixed gases under the conditions of the throat tube bundle, the working fluid is set to be water, the eliciting fluid is set to be air, the length of the throat is taken as 90 mm, 100 mm, 120 mm, 150 mm, 180 mm in turn, the working fluid feeding velocity $v_g = 2$ m/s, each simulation is computed for 3 s, and the gas volume distribution cloud diagrams are shown in Fig. 3-13 for the different lengths of the throat. Gas volume distribution cloud diagram, as shown in Fig. 2-11.

From Fig. 2-11, it can be seen that the length of the throat does not affect the ejection capacity of the jet device, but there is a minimum length of the throat for the gas-liquid mixing uniformity, when the length of the throat $L_h < 120$ mm (i.e., $12 D_z$), the gas in the throat cross-section of the volume fraction of the change is larger, indicating that this time the distribution of the gas is not uniform; when the length of the throat $L_h \geq 120$ mm, the closer the outlet of the throat, the volume fraction of the gas unchanged, indicating that the gas is coiled into the throat by the jet at a length of $12 D_z$, basically mixing uniformity. When the throat length $L_h \geq 120$ mm, the closer to the throat outlet, the gas volume fraction is basically unchanged, indicating that the gas is basically mixed uniformly at $12 D_z$ of the throat length after being sucked into the throat by the jet.

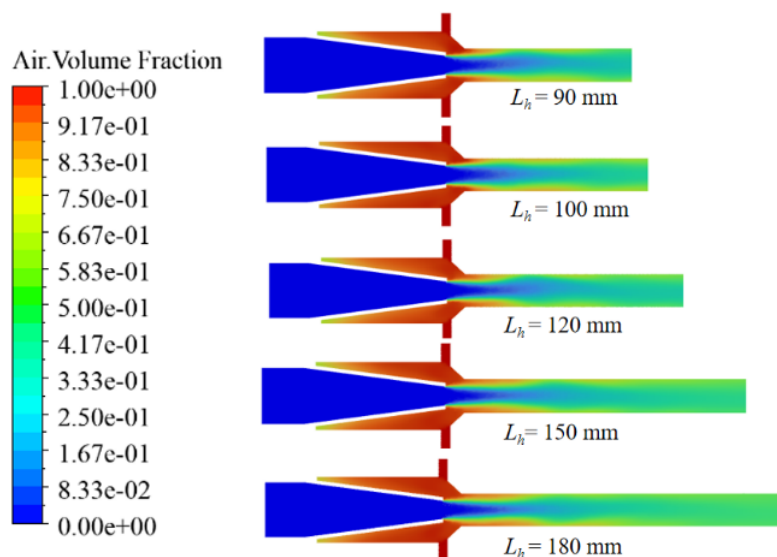


Fig. 2-11. Clouds of air volume fraction at different throat lengths

2.2.1.4. Effect of throat length on the flow field

As depicted in Fig. 2-12, the axial velocity cloud demonstrates variations under different throat lengths. The Fig. reveals that the morphology of the core area of jet velocity remains unaffected by throat length; however, there is inconsistency in the velocity distribution at the outlet of the pipe mouth for different throat lengths. When the pipe length is less than 100 mm, the flow velocity at the pipe outlet cross-section closely aligns with the axial velocity core area, indicating incomplete energy exchange between fluids. Moreover, there is inconsistency in flow velocities across each point of the orifice cross-section. Conversely, when the pipe length exceeds 150 mm, axial velocities at each point of the pipe outlet cross-section are essentially equal, suggesting completion of energy exchange between fluids. Insufficient mixing occurs when pipes are too short and weakens fluid velocity within excessively long pipes which hinders subsequent impact on impeller performance. Therefore, it is recommended to maintain a minimum pipe length of 120 mm ($12 D_z$) for comprehensive considerations.

Fig. 2-13 displays turbulence intensity cloud diagrams under varying throat lengths. It can be observed that changes in throat length do not affect turbulence intensity within fluid inside pipes significantly. Higher turbulence intensities primarily concentrate at nozzle outlets and for throat lengths below 120 mm; beyond this threshold value, turbulence intensity remains relatively stable

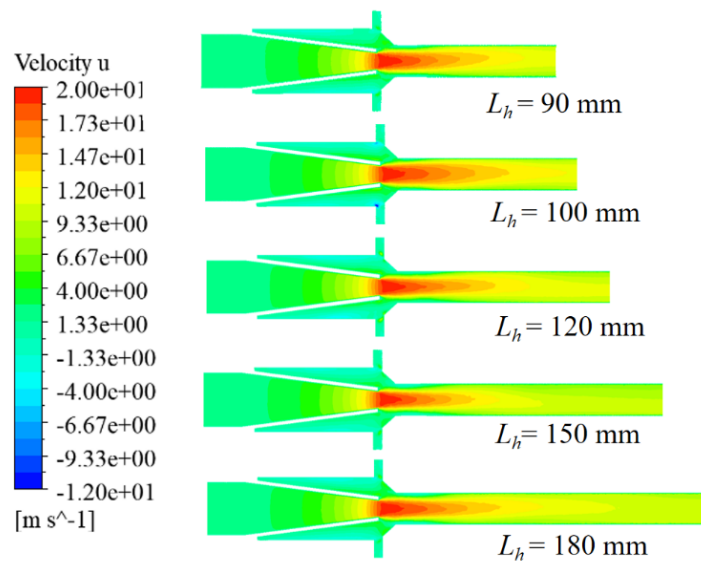


Fig. 2-12. Clouds of velocity u at different throat lengths

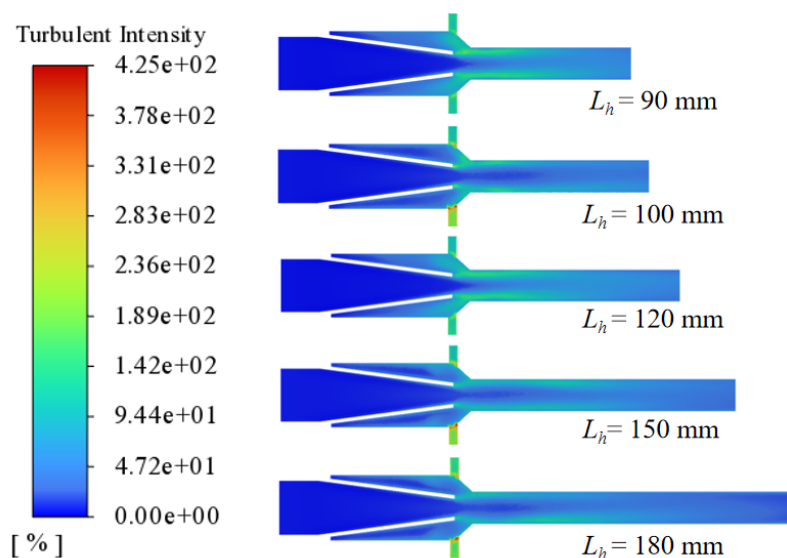


Fig. 2-13. Clouds of turbulent intensity at different throat lengths

Fig. 2-14 illustrates axial static pressure cloud diagrams for different throat lengths. From this Fig.'s analysis, it can be concluded that alterations in throat length have minimal impact on axial static pressure distribution within jet flow fields.; high-speed jet volume attraction jet fluid, in the throat inlet within a distance will also form a negative pressure zone, the length of the throat on the size of the negative pressure zone does not have an impact.

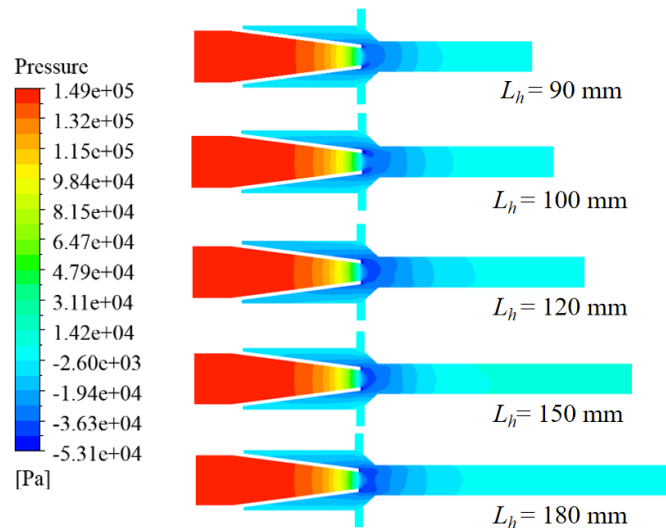


Fig. 2-14. Clouds of pressure at different throat lengths

2.2.2. Influence of the impact mixing link on the coiling and mixing capacity of the device

2.2.2.1. Impeller effect on gas dispersion

The impact mixing part is numerically simulated separately, with a gas volume fraction of 0.5 set in the inlet boundary condition to simulate the uniform bubble flow mixed by jet suction rushing into the vertical sleeve at a certain speed. The inlet velocity is set to 10 m/s to investigate the changes in gas-liquid distribution in the flow field with and without an impeller, as well as to understand the effect of impeller stirring on bubble shear distribution and determine whether combining jetting and stirring can enhance gas dispersion in the flow field.

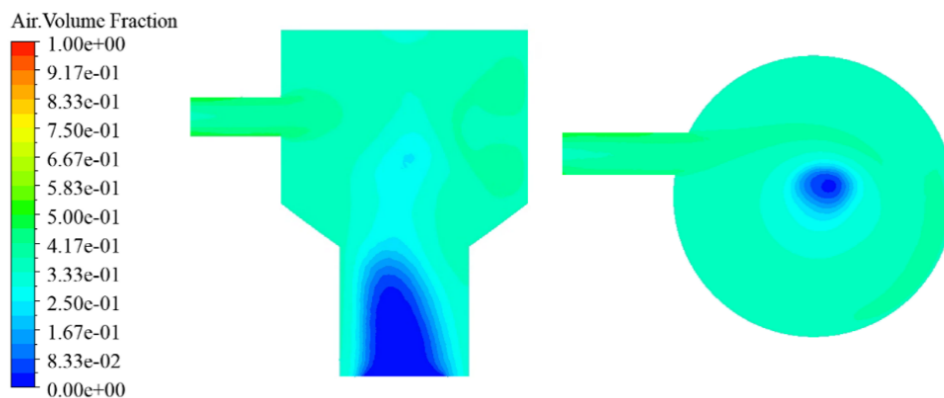


Fig. 2-15. Clouds of air volume fraction in the absence of impellers

When there is no impeller, Fig. 2-15 shows a cloud diagram of gas volume distribution in the impact flow field. It can be observed that without an impeller, when the uniform bubble flow enters the sleeve and collides with its cylindrical wall, it exits under gravity while experiencing helical flow which leads to a decrease in volume fraction. There is almost no gas distribution at the center of chamber liquid, and sharp decrease in gas volume fraction occurs at exit center where gases are concentrated only along boundary of flow bundle. This indicates that during flow and impact process, gas bubbles within flow beam merge resulting in reduced uniformity of their distribution.

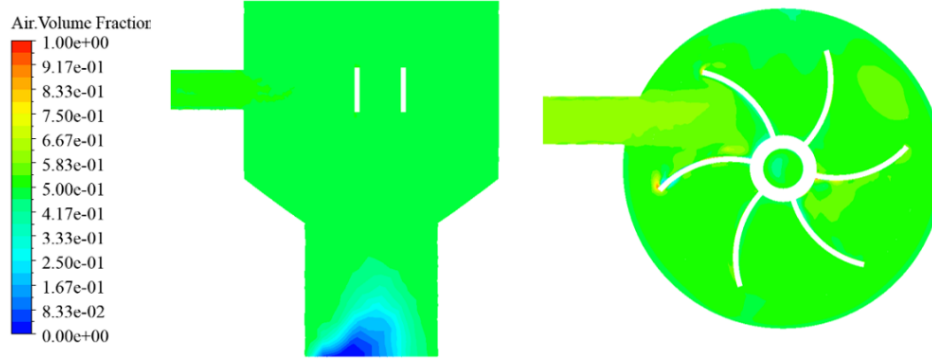


Fig. 2-16. Clouds of air volume fraction in the flow field with impeller

When there is an impeller, the cloud diagram of gas-liquid distribution within the impact stirring flow field is shown in Fig. 2-16. As can be seen from the Fig., the uniform bubble flow impact stirring impeller, by the impeller shear stirring effect, the gas in the sleeve is further shear dispersion, bubble volume fraction slightly increased, and ultimately in the gravity and centrifugal force downward out of the sleeve; the gas-liquid distribution within the entire chamber is relatively homogeneous, and the volume fraction of the gas at the exit of the center of the fluid decreases. It can be seen that the presence of the impact impeller can not only further shear bubbles, and promote bubble dispersion, but also help to maintain the stability of the volume fraction of gas in the flow bundle, reducing bubble merger.

2.2.2.2. Influence of impeller diameter on the mixing flow field

Other conditions remain unchanged, the chamber diameter of the model is fixed at $D_q = 120$ mm, and the impeller filling degree in the chamber is varied by changing the impeller diameter D_s (D_s is taken as 50 mm, 70 mm, 90 mm and 110 mm, respectively), to investigate the characteristics of the flow field under different impeller filling degrees.

The turbulence intensity cloud diagram under different impeller diameters is shown in Fig. 2-17. As can be seen from the Fig., the larger the impeller diameter, the more uniform turbulence intensity distribution inside the chamber; when the impeller diameter is smaller, the weaker the shear effect of the impeller on the jet beam, the more unfavourable for the uniform dispersion of the ejected fluid.

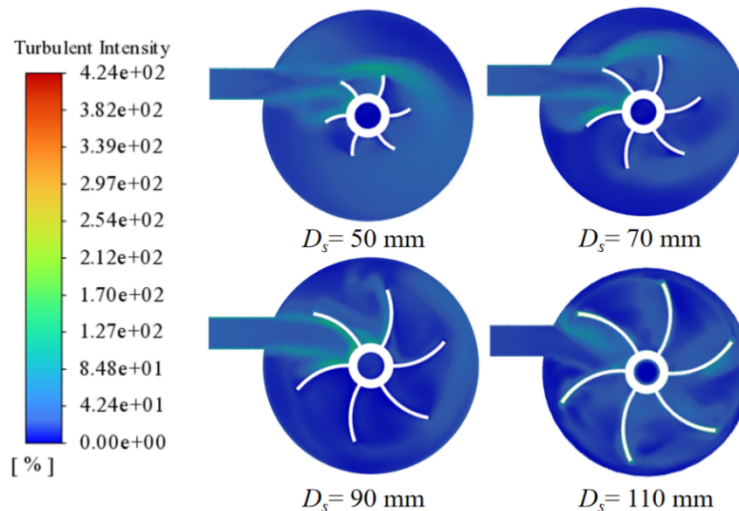


Fig. 2-17. Turbulence intensity cloud for different impeller diameters

The tangential velocity cloud under different impeller diameters is shown in Fig. 2-18. As can be seen from the Fig., the larger the impeller diameter, the larger the shear stirring effect on the fluid inside the chamber, the larger the tangential velocity difference of the fluid at each point inside the chamber;

the velocity difference at each point of the chamber cross-section reflects the motion state of the flow field, and the impeller diameter of 110 mm, the vortex will be formed between the impeller blades, which increases the turbulence of the field, and is conducive to the formation of small bubbles of the gas being sheared and broken.

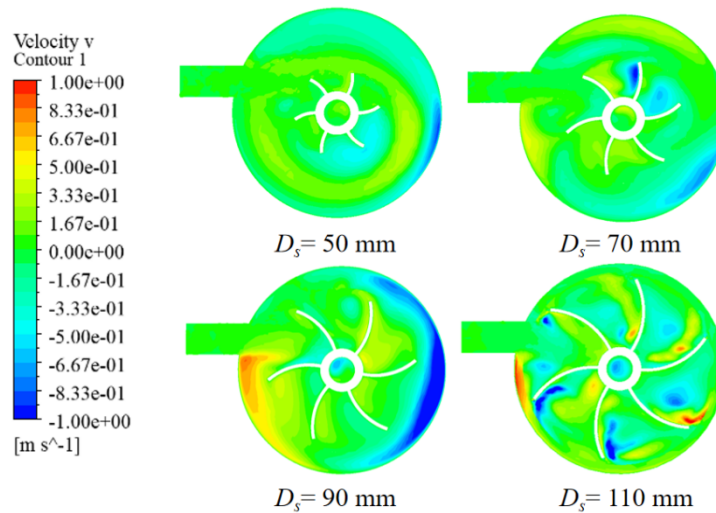


Fig. 2-18. Tangential velocity cloud for different impeller diameters

2.2.3. Effect of jet-stirring synergy on the coiling and mixing capacity of a device

In order to investigate the effect of the synergistic action of jet and stirring on the ejection capacity of the device, a certain rotational speed of the impact impeller is given during the simulation, and the change of the gas volume fraction inside the chamber is used as a reference to simulate the gas volume suction of the device under different nozzle outlet speeds, impact impeller stirring speeds, and the synergistic action of the two.

2.2.3.1. Influence of nozzle exit velocity on ejection capacity

The impeller mixing speed is controlled to be 60 r/min, the working fluid inlet speed is 1 m/s, 1.2 m/s, 1.6 m/s, 1.8 m/s (i.e., the corresponding nozzle outlet speeds are 9 m/s, 10.8 m/s, 12.6 m/s, and 14.4 m/s, respectively), and the working fluid is water, and the induced fluid is air, which are simulated respectively, and the volume fraction of the gas in the mixing chamber is used as a reference index, simulate and calculate the change of chamber gas volume fraction within 3 seconds, and export the data for graphing, as shown in Fig. 2-19.

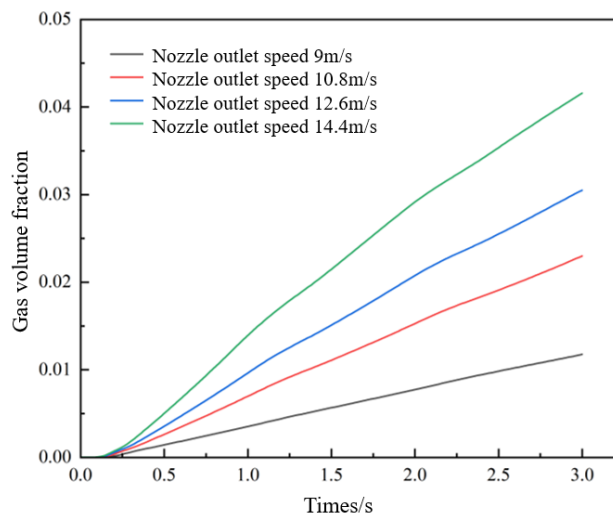


Fig. 2-19. Gas volume fraction diagram at different jet velocities

As can be seen from Fig. 2-19, there is a positive correlation between the nozzle outlet velocity and the suction volume, with the increase of jet velocity, the gas volume fraction inside the mixing chamber increases under the same operating time, and the increase of nozzle outlet velocity is conducive to the enhancement of the device's elicitation capacity.

2.2.3.2. Influence of impeller mixing speed on ejection capacity

Control the working fluid inlet velocity of 1 m/s, stirring speed was taken as 60 r/min, 75 r/min, 150 r/min, 225 r/min, and 300 r/min for simulation, and the gas volume fraction inside the stirring chamber was used as the reference index to simulate the change of chamber gas volume fraction within 3 seconds, as shown in Fig. 2-20.

From Fig. 2-20, it can be seen that the gas volume fraction inside the stirring chamber under the same operation time decreases gradually when the stirring impeller speed increases, indicating that the suction capacity of the device is weakened at this time and the suction volume decreases. The increase of stirring impeller speed has an inhibitory effect on the device elicitation capacity.

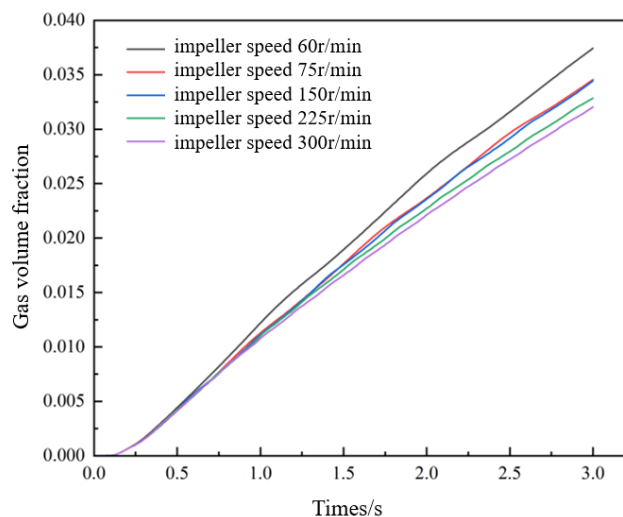


Fig. 2-20. Gas volume fraction diagram at different impeller velocities

2.2.3.3. Influence of the synergistic action of jet and agitation on the priming capacity of the device

The jet intensity is varied by changing the inlet velocity of the working fluid, in which the working fluid flow velocity is taken as 1 m/s, 1.2 m/s, 1.4 m/s, 1.6 m/s (i.e., corresponding to the nozzle outlet velocity of 9 m/s, 10.8 m/s, 12.6 m/s, and 14.4 m/s, respectively), and the impeller stirring rotational speed is taken as 60 r/min, 120 r/min, and 180 r/min, 240 r/min were simulated. The gas volume fraction size inside the device after 3 seconds of operation was used to characterize the suction capacity of the device, and the data were processed and the nozzle exit velocity-gas volume fraction plots at different stirring speeds were plotted, as shown in Fig. 2-21.

As can be seen from Fig. 2-21, the nozzle outlet speed is the main factor affecting the device elicitation capacity. In the smaller jet speed, the impeller speed changes on the device suction capacity of the larger, with the impeller stirring speed becomes larger, the device gas volume fraction decreases, the impeller growth rate will have an inhibitory effect on the device elicitation capacity; with the nozzle outlet speed continues to increase, the impeller speed changes on the device suction capacity of the influence of the device is gradually weakened, when the nozzle outlet speed of 14 m/s, increase the impeller rotation speed, the device When the nozzle outlet speed is 14 m/s, increasing the rotational speed of the impeller, the gas volume fraction in the device is basically unchanged. It can be seen that, when the nozzle outlet speed is greater than 14 m/s, the device suction capacity is dominated by the jet, and when the jet speed increases, the device suction capacity is enhanced, and the inhibitory effect of the stirring impeller on the device's ability to induce injection disappears.

Simultaneously increasing the jet velocity and the stirring velocity, the gas volume fraction inside the chamber increases, indicating that the effect of the jet velocity on the nozzle suction capacity is

greater than the inhibitory effect of the stirring impeller on it, and the suction capacity of the device is increased. If the increase of the stirring speed is much larger than the increase of the jet speed, the inhibition effect of the stirring on the nozzle suction capacity is much larger than the promotion of the jet speed, and the nozzle suction capacity will be inhibited.

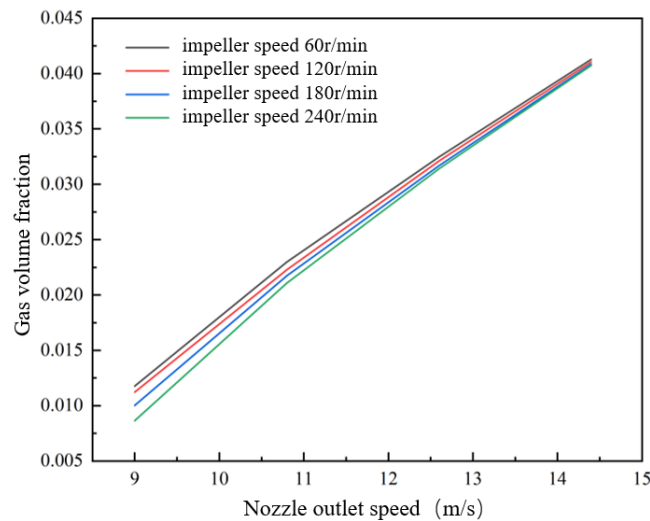


Fig. 2-21. Diagram of nozzle exit velocity-gas volume fraction at different stirring speeds

3. Mechanism of key link action in jet-stirring synergistic column flotation device

The laboratory physical model and test system of the jet-stirring synergistic column flotation device were constructed to prove the slurry conditioning effect of the device through the adsorption amount of chemicals on the surface of coal particles, and the absorbance test method was adopted, in which the absorbance of the supernatant of the slurry was measured under different conditions of slurry condition by changing the parameters of jet strength, throat length, and impeller fullness. The effect of jet-stirring synergism on slurry conditioning was obtained by the inverse inference of the relationship between the absorbance and the concentration of the chemical agents. Through the relationship between the absorbance and the concentration of the agent, the adsorption amount of the agent on the surface of the coal particles was inversely deduced, and the influence of the jet-stirring synergy on the slurry conditioning effect was obtained.

3.1 Test system

The jet-stirring synergistic column flotation device test system is shown in Fig. 3-1. As shown in Fig. 3-1, the test system mainly consists of a screw pump, a working fluid storage tank, a diverter/control valve, an electromagnetic flow meter, a jet-stirring mixing device, a stirring impeller, and a stirring tank. The key structural and operational parameters of the jet-stirring mixing device are: nozzle diameter $D_z = 10$ mm (area ratio $Ar = 3.24$), suction pipe diameter $D_x = 10$ mm; the throat is a custom-made high-transparency acrylic plate, with lengths ranging from short to long, with a minimum of 100 mm and a maximum of 1,000 mm; small holes are opened every 50 mm on the 1,000-mm throat as slurry sampling points; the nozzle and the throat are separable from each other; the impeller is 100 mm in diameter. The working fluid (slurry/water) is pumped into the subsequent jet mixing unit by a screw pump with a rated flow rate of 10 m³/h. In practice, the feed volume is controlled by a diverter valve and a control valve.

3.2. Influence of jet mixing synergy on the effect of stock conditioning

In the actual coal slurry flotation process, the dosage of the flotation collector typically between 800 g/t ~ 1500 g/t. However, directly adding the collector into the slurry results in poor mixing, chemical dispersion, and overall effectiveness., and thus the gas or liquid with the chemical way of suction mixing. In this thesis, a trapping agent dosage of 1000 g/t was used along with a slurry concentration of 60 g/L. The agent was added through gas injection at a fixed height above the injection pipe to ensure

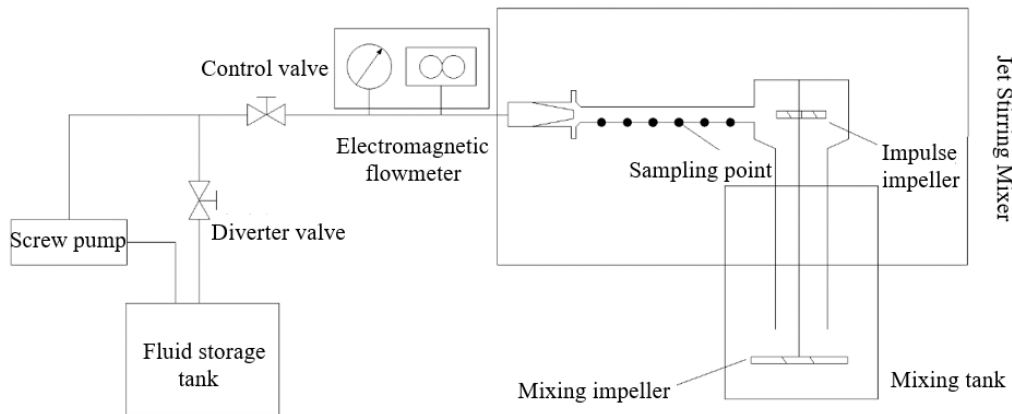


Fig. 3-1. Test system for jet-stirring synergistic column flotation device

uniform distribution. The study focused on investigating the synergistic effect of jet-impact mixing link in a test system using a jet-impact mixing column device for coal slurry mixing under different conditions (passive rotation of impact impeller). This key link plays an important role in promoting collision and adhesion between coal slurry particles and chemical agents. At the end of each pulping test, 500 mL of slurry was collected and left undisturbed for 12 hours. A certain amount of supernatant was then extracted from which absorbance measurements were taken using an ultraviolet spectrophotometer. By extrapolating backwards from paraffin content in the supernatant, corresponding adsorption amounts of coal slurry and chemicals were determined

3.2.1. Effect of jet strength on the adsorption of flotation chemicals or agents

By controlling the valve to change the amount of feed to control the intensity of the jet, the suction volume is fixed at 600 L / h, in a jet slurry mixing cycle T ($1T = 1$ min), uniformly add the trapping agent paraffin, the dosage of 1000 g / t, 25 L slurry trapping agent dosage of a total of 1.875 mL; each time the end of the mixing of the slurry, 500 mL of the slurry, the supernatant liquid volume of 100 mL taken after 12 hours of rest, and Add 0.1 g Sudan red III and 50 mL of anhydrous ethanol, stir for 5 min, leave for 3 min, take a sample to measure the absorbance and record the data. The effect of different feeding volume, i.e., jet strength, on the adsorption amount of the agent is shown in Figs. 3-2.

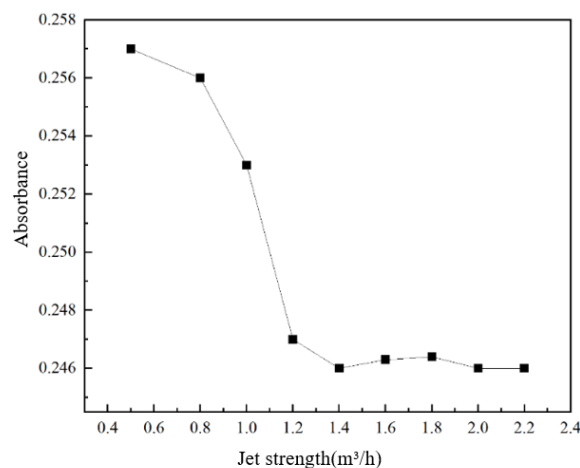


Fig. 3-2. Effect of jet strength on the adsorption of flotation chemicals or agents

As can be seen from Fig. 3-2, with the increase of jet strength, the absorbance of slurry supernatant gradually decreases, the feed volume is greater than 1.4 m³/h, the absorbance of supernatant basically no longer change; when the feed volume is equal to 1.4 m³/h supernatant absorbance is the smallest, i.e., the coal slurry with the maximum amount of chemical adsorption, the adsorption effect is the best. It can be seen that the greater the jet strength, the greater the adsorption amount of chemicals, and the

better the effect of slurry adjustment, when the jet strength increases to a certain extent, the adsorption amount of coal slurry and chemicals tend to stabilize, no longer with the increase in jet strength and change.

3.2.2. Effect of throat length on the adsorption of flotation chemicals or agents

By manipulating the valve to regulate the feed amount and control the jet intensity, a fixed suction volume of 600 L/h is maintained. During a single cycle of slurry mixing ($T = 1$ min), paraffin trapping agent is uniformly added at a dosage of 1000 g/t, resulting in a total dosage of 1.875 mL for every 25 L of slurry. At the end of each mixing cycle, after allowing for a rest period of 12 hours, 500 mL of slurry is taken and then subjected to supernatant liquid extraction with an additional volume of 100 mL. To this extracted supernatant liquid, Sudan red III (0.1 g) and anhydrous ethanol (50 mL) are added followed by stirring for 5 minutes and subsequent resting for another 3 minutes before taking samples to measure absorbance values. The absorbance of agents with different throat lengths is shown in Fig. 3-3.

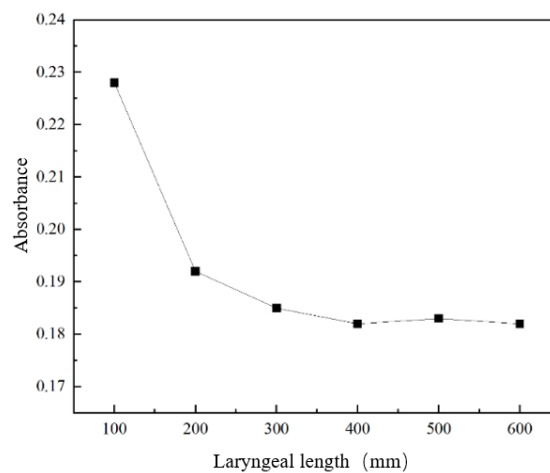


Fig3-3 Effect of different throat lengths on the adsorption of pharmaceutical agents

As can be seen from Fig. 3-3, the absorbance of the supernatant was higher when the length of the pipe was 100 mm, and the absorbance gradually decreased with the increase of the length of the pipe, and tended to be stable after 300 mm, indicating that the adsorption of coal sludge and chemicals was basically completed at the position of the length of the pipe of 300 mm (i.e., 30 Dz).

3.2.3. Influence of impeller fullness on the adsorption of flotation chemicals or agents

Impeller fullness is the ratio of the diameter of the impact impeller to the diameter of the external sleeve. In the actual test, combined with the existing conditions in the laboratory, the impeller fullness is achieved by changing the size of the sleeve diameter.

Adopt gas-induced injection to bring in the agent, the suction volume is fixed at 600 L/h, in a jet slurry adjustment cycle T ($1T=1$ min), uniformly add the trapping agent paraffin, the amount of 1000 g/t (25 L slurry, the amount of trapping agent total 1.875 mL), change different impeller filling degree for slurry adjustment test, each time the end of the slurry adjustment, take 500 mL of slurry, let it stand for 12 hours, and take the supernatant liquid volume of 100 mL. After each slurry adjustment, 500 mL of the slurry was taken and left for 12 hours, 100 mL of supernatant was taken, 0.1 g of Sudan red III and 50 mL of anhydrous ethanol were added, stirred for 5 min, and then left for 3 min, and the samples were taken to measure the absorbance. The effect of different impeller filling degree on the adsorption amount of the agent is shown in Fig. 3-4.

As can be seen from Fig. 3-4, the larger the impeller fullness is, the smaller the absorbance is, that is, the larger the adsorption amount of the agent is, and the better the effect of collision adhesion between the coal slurry and the agent is. Impeller fullness is too small, the supernatant measured in the absorbance is larger, indicating that the impeller fullness is too small is not conducive to the coal slurry and the full adsorption of the agent; impeller fullness is greater than 70%, the absorbance in the

supernatant decreases, continue to increase impeller fullness, absorbance changes in the magnitude of the smaller, when the impeller fullness of 83% of the absorbance of the lowest, when the coal slurry agent adsorption is the largest amount of the adsorption, the adsorption effect is the best; Impeller fullness is greater than 90% of the absorbance slightly. When the impeller fullness is greater than 90%, the absorbance increases slightly. From the Fig., it can be concluded that the impeller filling degree of the impact stirring impeller should not be too small or too large, and it is most suitable to keep it between 70% and 85%.

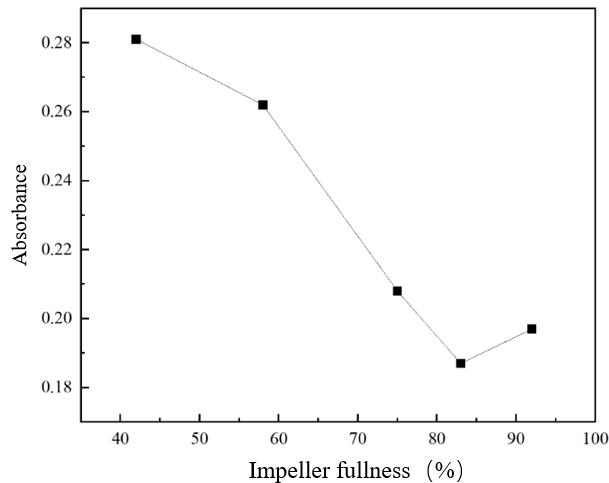


Fig. 3-4. Influence of impeller fullness on the adsorption of pharmaceuticals

4. Test verification of the pulping effect

4.1. Test methods

The fixed structural parameters of the jet-stirring mixing device remain unchanged. The throat length is a 150 mm acrylic tube, and the impact impeller diameter is 50 mm. The external sleeve has been modified to ensure that the impeller is filled to 60%. Additionally, adjustments have been made to the diverter valve and control valve in order to control the incoming material flow rate at $Q = 2.03 \text{ m}^3/\text{h}$. For flotation testing, paraffin is used as the collector with a dosage of 1000 g/t, while methyl isobutyl methanol serves as the frother with a dosage of 120 g/t. The slurry concentration is set at 60 g/L, and a complete slurry cycle takes approximately $T = 1 \text{ min}$.; slurry adjustment is divided into a single jet slurry adjustment and jet-impact stirring synergistic slurry adjustment, a single flotation slurry adjustment test, the throat and fluid collection tank is connected to the jet - the For the single flotation slurry adjustment test, the pipe is connected to the fluid collection tank, and for the jet-impact stirring synergistic slurry adjustment test, the pipe is connected to the stirring part; the trapping agent is uniformly fed by the gas injection method.

The slurry will be introduced into the flotation machine for flotation test after slurry mixing in different ways, and the flotation test will be carried out in accordance with GB/T 4757-2001, and no more steps for adding trapping agent are carried out, the slurry will be introduced into the flotation machine and stirred for 1 min and then added with a foaming agent, and the valve will be opened to blow gas for scraping after stirring for 10 s. After scraping for 3 min, and then the flotation will be carried out. The refined coal was filtered and dewatered, dried, and the ash content was measured. Change the slurry cycle to 0.5T, 1T, 1.5T, 2T, and 2.5T, and repeat the above test steps to investigate the optimal slurry cycle time under different slurry adjustment methods. The test was preceded by a unit flotation test, and the test results were analyzed together for comparison.

4.2. Analysis of test results

According to the unit flotation, single jet slurry flotation, jet beam-impact stirring synergistic slurry flotation and different slurry circulation times under the jet beam-impact stirring synergistic slurry flotation were tested, and the comparison of the results of the jet-impact stirring synergistic slurry flotation tests with different slurry circulation times were shown in Fig. 4-1.

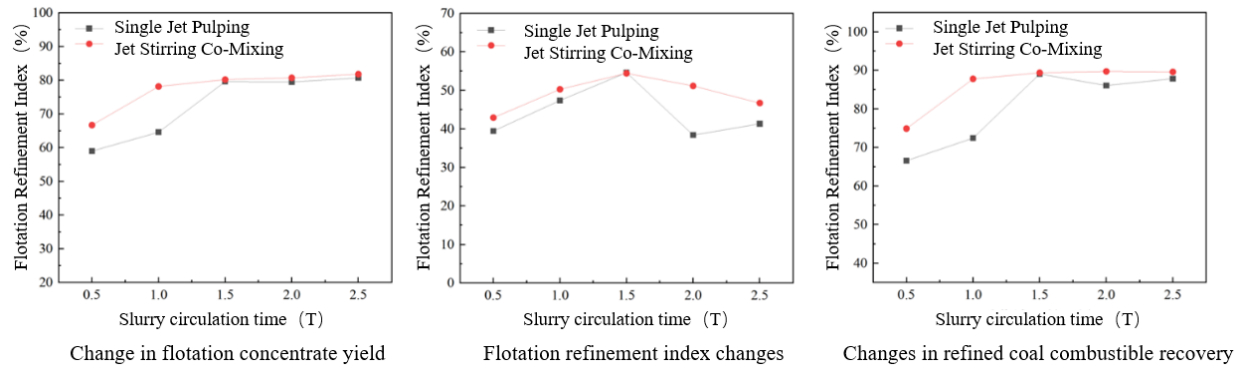


Fig. 4-1. Influence of slurry circulation time on the flotation effect of different regulated slurry flow fields

Compared to single-jet slurry flotation, jet-stirring synergistic slurry flotation exhibits superior performance in terms of flotation concentrate yield, flotation perfection index, and fine coal combustible recovery. This suggests that jet-stirring synergistic slurry flotation enhances the effectiveness of slurry flotation more effectively than single-jet slurry flotation. When the slurry circulation time is 1.5T ($T = 1$ min), both types of slurry flotation achieve the highest values for fine coal yield, flotation perfection index, and fine coal combustible recovery rate. Furthermore, as the slurry circulation time continues to increase beyond this point, there is minimal change observed in the fine coal yield during flotation. This indicates that after 1.5 cycles of circulating through the system, the optimal adherence between the floatants and slurries has been achieved.

5. Conclusions

- (1) Numerical simulation indicates that the suction mixing ability of the jet device is significantly influenced by the nozzle exit velocity. When the nozzle exit velocity (v) is less than 3.6 m/s, the intensity of the jet is insufficient, which hinders bubble rupture and dispersion. In the range of 7.2 m/s $< v < 18$ m/s, the elicitation ability and gas suction dispersing ability of the jet device gradually improve. When $v \geq 18$ m/s, the elicitation ability reaches its limit. The throat length does not affect ejection capacity but a minimum throat length of $12 D_z$ ensures uniform mixing for two fluid streams. At lower jet velocities, impeller growth rate inhibits ejection capacity; however, with increasing nozzle exit velocity, impeller speed has a diminishing influence on suction capacity until it becomes negligible when $v > 14$ m/s and dominated by jet action.
- (2) The adsorption amount of agents increases with higher jet strength in slurry adjustment processes leading to better effects. However, after reaching a certain degree ($Q = 1.4 \text{ m}^3/\text{h}$ at $v = 5.0$ m/s), coal slurry and agent absorption tends to stabilize and no longer changes with further increase in jet strength. The throat length should not be less than 100 mm as measured absorbance tends to stabilize after approximately 300 mm indicating completion of coal sludge and chemical adsorption at this position ($30 D_z$). The larger the filling degree of the impact impeller in the impact chamber, the better the effect of collision adhesion between coal slurry and chemicals, but when the impeller is too small, it is not conducive to the full adsorption of coal slurry and chemicals; the filling degree of the impeller of the impact mixing impeller should not be too small or too large, and it is best to keep it between 70% and 85%.
- (2) Both single-jet slurry mixing and jet-impact stirring synergistic slurry mixing methods have strengthened the effect of coal slurry mixing; compared with single-jet slurry mixing, the jet-stirring synergistic slurry mixing method can strengthen the effect of slurry mixing more than single-jet slurry mixing, and the flotation effect is better. The flotation chemicals and slurry were fully adhered to each other after 1.5 cycles of slurry circulation, and the optimal slurry circulation time was 1.5 T. The flotation chemicals and slurry were fully adhered to each other after 1.5 cycles of slurry circulation.

References

- BU, X., ZHOU, S., SUN, M., et al, 2021. Exploring the relationships between gas dispersion parameters and differential pressure fluctuations in a column flotation. *ACS omega*, 6(34): 21900-21908.

- GE, S.R., WANG, B., FENG, H.H., 2023. *Dynamic Carbon Neutral Modelling of Coal-Based Energy Sources and Assessment of Their Carbon Reduction Benefits in Supply Conservation*. Chinese Academy of Engineering Sciences, 25(05):122-135.
- GUO, J., LI, W.M., Y, X.Y., 2015. *Analysis of world coal resources supply and demand*. China Coal, 41(12):124-129.
- HAN, Y., ZHU, J., SHEN, L., et al, 2019. *Bubble size distribution characteristics of a jet-stirring coupling flotation device*. Minerals, 9(6): 369.
- HUANG, G., XU, J.Q., LI, K.Z., et al, 2022. *Mechanism of fine-grained coal slurry flotation enhanced by slurry conditioning*. Coal Journal, 47(S1):246-256.
- LI, Y.J., CUI, G.W., WANG, J.Q., 2010. *Current status and development of coal slurry flotation chemicals*. Coal Processing Technology, (05):68-70+6.
- LI, J.H., MA, L.Q., CHENG, G., et al, 2014. *Research Progress of Coal Slurry Flotation and Slurry Conditioning Technology and Equipment*. Coal Engineering, 46(09):109-111+115.
- LI, S., WANG, Y., LU, D., et al, 2020. *Improving separation efficiency of galena flotation using the Aerated Jet Flotation Cell*. Physicochemical Problems of Mineral Processing, 56(3): 513-527.
- LI, M., XU, M.D., JIN, W., 2019. *Experimental study of the effect of diesel oil on the stability of flotation froths*. Coal Journal, 44(06):1876-1882.
- MIAO, X.X., QIAN, M.G., 2009. *Research Status and Prospect of Green Mining of Coal Resources in China*. Journal of Mining and Safety Engineering, 26(01):1-14.
- NATIONAL BUREAU OF STATISTICS., 2024. *Statistical Bulletin of the People's Republic of China on National Economic and Social Development*, 2023.
- SAFARI M., HOSEINIAN F S., DEGLON D., et al, 2020. *Investigation of the reverse flotation of iron ore in three different flotation cells: Mechanical, oscillating grid and pneumatic*. Minerals Engineering, 150: 106283.
- SCHWARZ M P., KOH P T L., WU J., et al, 2019. *Modeling and measurement of multi-phase hydrodynamics in the Outotec flotation cell*. Minerals Engineering, 144: 106033.
- SHI, W.D., YE, Z.M., LIU, J.R., et al, 2006. *Numerical simulation of the inlet flow field of a new jet self-priming pump*. Journal of Agricultural Machinery, (10):50-52+61.
- SUN, X.D., ZHANG, B., PENG, S.P., 2020. *Research on the development trend and strategic countermeasures of China's clean coal technology 2035*. Chinese Academy of Engineering Sciences, 22(03):132-140.
- WANG, H.N., 2019. *Study on energy distribution and bubble dispersion characteristics of annular jet flotation device*. Anhui University of Science and Technology.
- WANG, S.M., SHEN, Y.J., SONG, S.J., et al, 2023. *Changes in the status of coal energy and green low-carbon development under the "dual-carbon" target*. Coal Journal, 48(07):2599-2612.
- WANG, C., WANG, C., YU, A., et al, 2021. *Effect of closure characteristics of the annular jet mixed zone on inspiratory performance and bubble system*. Processes, 9(8): 1392-1392.
- WANG, H., YANG, W., YAN, X., et al, 2020. *Regulation of bubble size in flotation: A review*. Journal of Environmental Chemical Engineering, 8 (5): 104070.
- XIA, Y., RONG, G., XING, Y., et al, 2019. *Synergistic adsorption of polar and nonpolar reagents on oxygen-containing graphite surfaces: Implications for low-rank coal flotation*. Journal of Colloid and Interface Science, 557: 276-281.
- XU, H.X., YU, P., TIAN, H., et al, 2023. *Current status and outlook of the research and application of the jet pulping method*. Coal Technology, 42 (02): 229-232.
- YANG, Y.B., QU, J.Z., ZHU, Z.Q., 2021. *Progress of whole-process treatment technology for difficult-to-settle coal slurry water*. Clean Coal Technology, 27(05):106-114.
- YUAN, L., 2017. *Scientific Concept of Precision Coal Mining*. Journal of Coal, 42(01):1-7.
- ZHANG, B., PENG, S.P., WANG, D., et al, 2019. *Research on the Strategic Path and Countermeasures for Building a Strong Coal Resource Country*. Chinese Academy of Engineering Sciences, 21(01):88-96.
- ZHANG, Y.S., DONG, T., XIAO, Y., et al, 2021. *Current status of China's energy production, consumption and energy storage and the trend of change under carbon-neutral conditions*. Science Bulletin, 66(34):4466-4476.
- ZHOU, M., 2023. *Analysis of the Transformation and Development of China's Coal Industry under the Background of "Dual Carbon"*. Coal Economic Research, 43(08):52-59.
- ZHOU, W., 2019. *Optimization of slurry flow field by jet and study on the mechanism of action of the collector in slime region*. Anhui University of Science and Technology.
- ZHU, Y.M., 2022. *Advances in Flotation Pharmaceuticals 2021*. Non-ferrous metals (mineral processing component), (02):1-15
- ZHU, H., ZHU, J., VALDIVIESO A L., et al, 2019. *Study on flow behaviour in the Short-Throat-Jet type flotation machine*. Current Science, 116(4): 592-596.